

Article

Design and Implementation of a Digital Angular Rate Sensor

Li-Feng Wu ^{1,*}, Zhen Peng ² and Fu-Xue Zhang ³

¹ Beijing Engineering Research Center of High Reliable Embedded System, Capital Normal University, Beijing, 100048, China

² Department of Computer, North China Institute of Science and Technology, Beijing, 101601, China; E-Mail: zhen_peng1981@163.com

³ Research Center of Sensor Technology, Beijing Information Science & Technology University, Beijing, 100101, China; E-Mail: zhangfuxue@263.net

* Author to whom correspondence should be addressed; E-Mail: wooleef@gmail.com; Tel.: +86-10-68906706; Fax: +86-10-68906706.

Received: 23 August 2010; in revised form: 8 October 2010 / Accepted: 9 October 2010 / Published: 28 October 2010

Abstract: With the aim of detecting the attitude of a rotating carrier, the paper presents a novel, digital angular rate sensor. The sensor consists of micro-sensing elements (gyroscope and accelerometer), signal processing circuit and micro-processor (DSP2812). The sensor has the feature of detecting three angular rates of a rotating carrier at the same time. The key techniques of the sensor, including sensing construction, sensing principles, and signal processing circuit design are presented. The test results show that the sensor can sense rolling, pitch and yaw angular rate at the same time and the measurement error of yaw (or pitch) angular rate and rolling rate of the rotating carrier is less than 0.5%.

Keywords: gyroscope; accelerometer; pitch; yaw; angular rate

1. Introduction

In recent years, MEMS sensors have become more and more popular in the industrial and automotive fields. Because the MEMS angular rate sensors have the characteristics of high performance, extremely compact size, low power operation and low cost, they have been considerable interest in their design and fabrication [1,2]. Currently, there are many micromechanical gyroscopes (angular rate sensors), including electrostatically driven [3,4], electromagnetic driven [5-7] and

piezoelectric driven [8,9] ones, *etc.*, designed to measure the angular rate or the rotation angle by integrating the measured angular rate with respect to time. These gyroscopes have drive parts and sensing parts, so their structures are complex. We are investigating a novel MEMS-based gyroscope, which has no driving parts, and utilizes the circumrotation of the rotating carrier itself as driving force. Therefore, it is suitable for detecting the angular rate of a rotating carrier due to its characteristics.

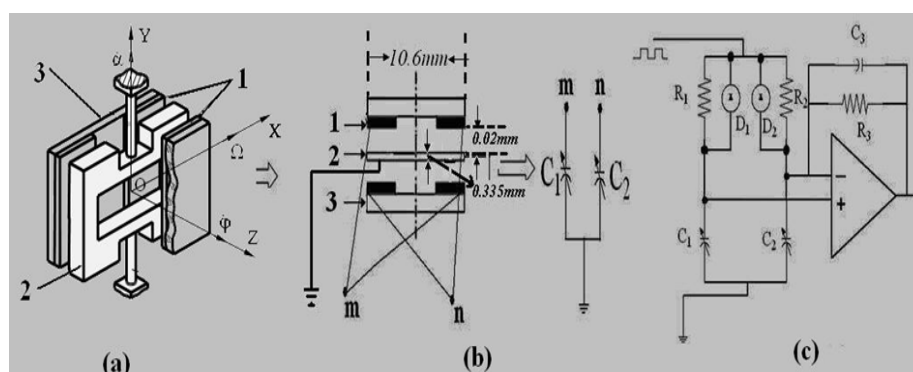
The design, fabrication and basic performance of the gyroscope have been reported in [10]. Moreover, we have shown that rotating carrier rotational velocity instability influences the output signal, and presented a method to eliminate the effect in actual applications [11]. Now, based on the sensing element, a novel digital angular rate sensor is proposed. It includes sensing elements and signal processing circuits. The digital angular rate sensor can sense three angular rates of a rotating carrier and output three digital angular rate signals.

2. The Sensing Element and Operating Principles

2.1. Sensing Element

The structure of the sensing element is shown as Figure 1(a). It consists of a silicon four leaf clover structure. The silicon pendulum is obtained through bulk micromachining technology and attached to the center. It can form two pairs of capacitances with the opposite copper plating ceramic substrate, respectively.

Figure 1. The structure and signal processing of the sensing element: (a) lateral view of the structure of sensing element, 1-the copper electrode, 2-the silicon pendulum, 3-the ceramic substrate; (b) the differential-capacitance; (c) the C/V transformed circuitry.



The dimensions of the sensing element are illustrated in Figure 1(b). The silicon pendulum is connected with an analog ground, and the four pieces of copper plating ceramic substrate are connected together, as shown in Figure 1(b). Thus we can obtain a pair of differential capacitors, shown in Figure 1(b), right. Figure 1(c) is the corresponding C/V transformed circuitry. It is clear that the capacitance of these four capacitors varies with the angle velocity Ω . When the change of differential capacitance is small it is easily disturbed by the distributed capacitance, while in the pick-up circuit, the alternating-current bridge is used as the interface of the transfer circuit. The differential capacitance is discharged and charged by a square wave pulse current, then amplified by amplifier, finally the output voltage signal, which is directly proportional to the angle velocity Ω , is obtained.

2.2. Sensing Principle

The sensing principle of the sensing element is based on the measurement of Coriolis forces. From Figure 1(a), the sensing element is installed on a rotating carrier and rotates together with the rotating carrier along the OZ axis. Once the rotating carrier has a yaw or a pitch angular rate (along the OX or OY axis direction), the silicon pendulum swings around the internal sensitive OX axis under the Coriolis forces. Therefore, the differential capacitance C_1 , C_2 can sense yaw or pitch angular rate. According to the C/V transformed circuitry, as shown in Figure 1(c), we can obtain:

$$u_o = f(\dot{\varphi})\Omega\sin(\dot{\varphi}t + \theta_1(t)) \quad (1)$$

where $\dot{\varphi}$ is the rolling frequency of rotating carrier, Ω the fused yaw and pitch angular rate, u_o the output voltage, $\theta_1(t)$ the initial phase, $f(\dot{\varphi})$ the transmission factor, which depends on the $\dot{\varphi}$. In order to eliminate the effect of $\dot{\varphi}$, according to the method [11], u_o can be expressed as u_1 as follows:

$$u_1 = k\Omega\sin(\dot{\varphi}t + \theta_1(t)) \quad (2)$$

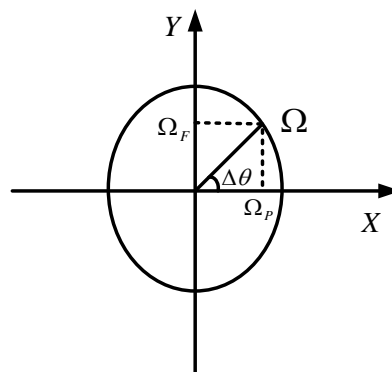
where k is the scale factor. From the function (2), it is clear that the virtual value of output voltage is directly proportional to the synthesis of angular rate Ω of rotating carrier between yaw and pitch.

In order to obtain yaw and pitch angular rate, an accelerometer is used, which is attached to the rotating carrier. The output of the accelerometer is:

$$u_2 = A\sin(\dot{\varphi}t + \theta_2) \quad (3)$$

where A is output max value of output, which depends on the rolling rate $\dot{\varphi}$, θ_2 is the initial phase. The frequency of the output signal is the same as the rotating carrier's rolling frequency. According to the study above, the synthesis angular rate of the rotating carrier is determined by measuring the phase difference between the signals of gyroscope and accelerometer. The relationships between Ω , Ω_p , Ω_F , and $\Delta\theta = \theta_1(t) - \theta_2$ are shown in Figure 2.

Figure 2. The relationships between Ω , Ω_p , Ω_F , and $\Delta\theta$.



Thus we can obtain the following expressions:

$$\Omega_p = U_1 \cos(\theta_1(t) - \theta_2) / k = U_1 \cos(\Delta\theta) / k \quad (4)$$

$$\Omega_F = U_1 \sin(\theta_1(t) - \theta_2) / k = U_1 \sin(\Delta\theta) / k \quad (5)$$

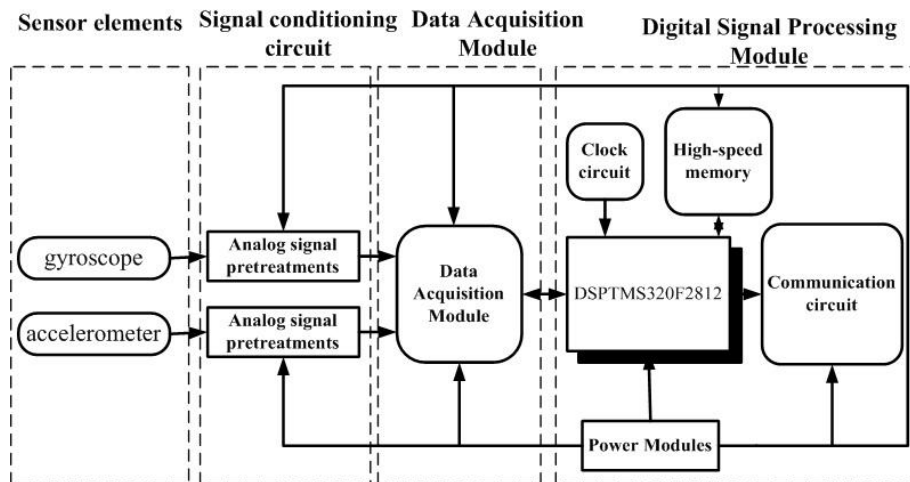
Here, Ω_F is pitch angular rate, Ω_p yaw angular rate, and U_1 the virtual value of u_1 .

3. Digital Circuits Design

3.1. Hardware Circuits Design

In order to implement all of the above-mentioned operations, we have designed signal-conditioning hardware circuits as shown in Figure 3. The hardware circuits consist of four parts: sensing elements, analog signals pretreatments, data acquisition module and signal demodulation processing circuits.

Figure 3. The signal-conditioning circuit diagram.



The first part includes two sensing elements: gyroscope and accelerometer, which sense the angular rate and the direction, respectively. The second part is used to deal with the analog signals of the sensing elements, including the gyroscope signal pretreatment circuit and the accelerometer pretreatment circuit, shown in Figure 4 and Figure 5, respectively. The gyroscope signal pretreatment circuit mainly consists of the regulated power supply, bridge circuit, pulse excitation, difference amplifier, band-pass filter demodulator and phase compensation, *etc.* It is capable of complete detection of small capacitances and transferring the capacitance into a voltage signal that ranges from -10 V to $+10\text{ V}$.

Figure 4. The gyroscope signal pretreatment circuit.

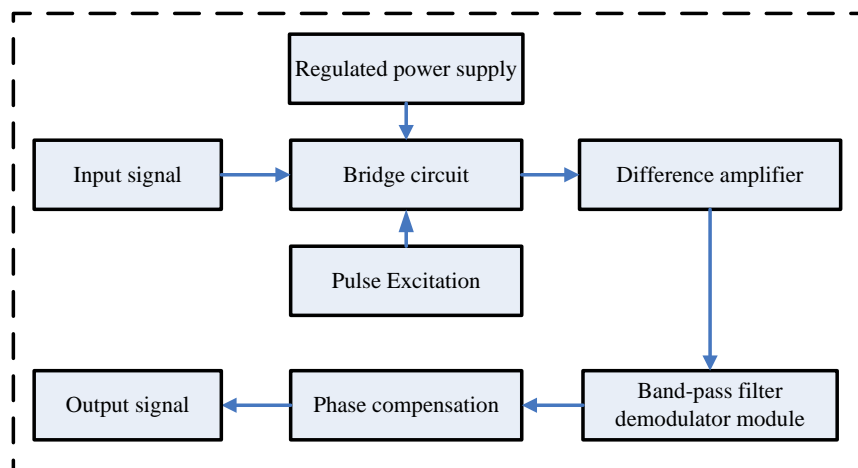
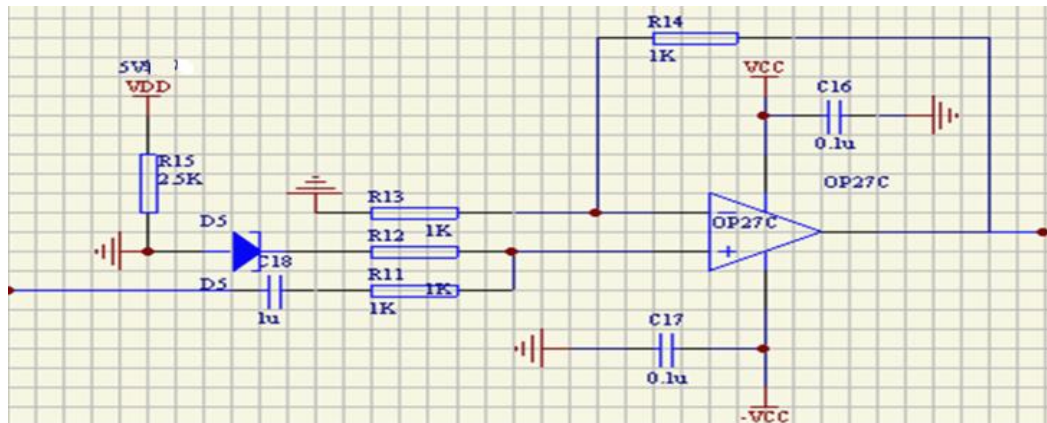
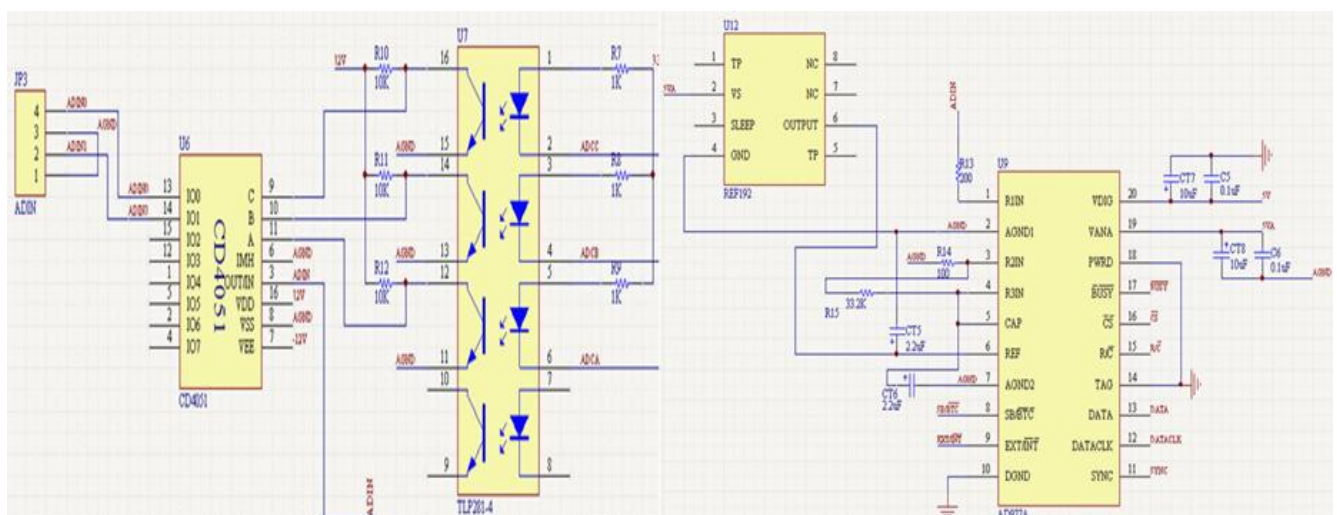


Figure 5. The accelerometer signal pretreatment circuit.

The output signal of the accelerometer contains DC component, which changes with different rotating rates. In addition to this, the output AC component of the accelerometer is weak, about $-0.25\text{ V}\sim+0.25\text{ V}$. To solve these problems, we use a capacitance (c18) to filter out the DC, then make up the output signal though an operational amplifier circuit to amplify it 10 times, coupled with a superimposed voltage of 2.5 V DC, so the output voltage is in the range $0\text{ V}\sim 5\text{ V}$.

The third part is data acquisition module as shown in Figure 6, which mainly consists of AD977A, CD4051 and TLP281-4. There are two input signals but AD977A only has one input port, so we designed a switch module. The CD4051 analog multiplexer is a digitally-controlled analog switch having low ON impedance and very low OFF leakage current; it is a single 8-channel multiplexer having three binary control inputs, A, B and C, and an inhibit input. The three binary signals select 1 of 8 channels to be turned on, and connect one of the 8 inputs with the output. A, B and C are controlled by TLP281-4 alternately to sample the gyroscope and accelerometer signals.

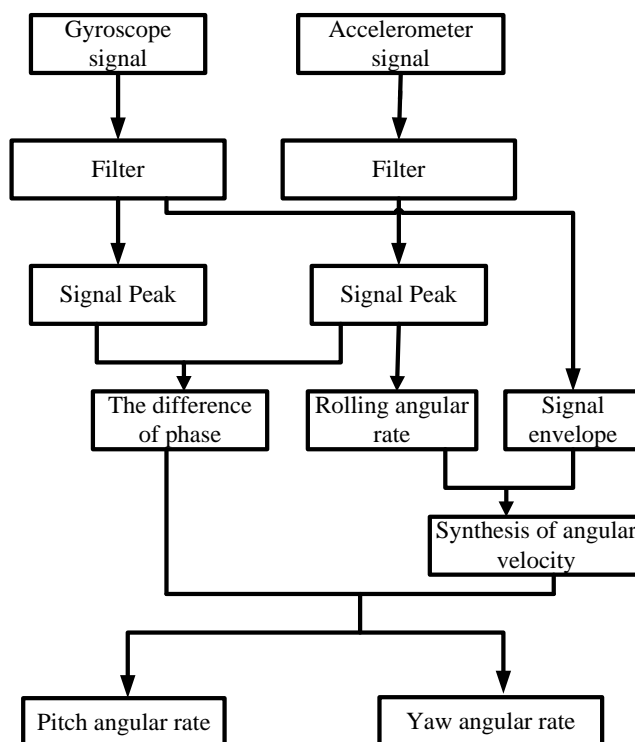
Figure 6. The data acquisition circuit.

The last part is the signal demodulation processing circuits based on DSP2812 and peripheral circuits. The peripheral circuits include power module, reset circuit and serial port communication circuit of DSP2812, *etc.* We use a MAX3232 chip as communication for UART output. The 5V power design is based on the LM2576 and the 1.8 V and 3.3 V voltage is transferred by using the LM1117.

3.2. Signal Processing Algorithm

The signal processing is shown in Figure 7. First, we can filter the signal and calculate the frequency of the sensing element (accelerometer) signal, which is same as the rotating carrier rolling rate; Secondly, we calculate the peak output voltage of the signals and get the phase difference between gyroscope and accelerometer. At the same time, we can obtain the envelop of the gyroscope signal, which is proportional to the fused angle rate of yaw and pitch. According to the phase difference between gyroscope signal and accelerometer signal, we can obtain yaw angular and pitch angular rate.

Figure 7. The signal-conditioning processing.



4. Test Results

The appearance of the digital angular rate sensor is shown in Figure 8. The device has the shape of a cylinder with a diameter of 5 cm and a height of 4 cm. The sensor can be mounted on a simulator of a rotating carrier system designed specifically to apply this sensor test. The system consists basically of a three-axis servo table. One is used to simulate the rotating carrier, and the others two control the attitude of the rotating carrier. The simulator rolls as a rotating carrier with yaw and pitch angular rate. The digital outputs are recorded by a computer. First of all, we set a rolling rate at 20 Hz, then set yaw and pitch angular vibration frequency as 1 Hz, vibration amplitude as 10° , respectively. The output results were recorded by the computer. Figures 9–11 illustrate the comparison between the measured angular rate and the actual rate.

Figure 8. The appearance of a new digital angular rate sensor.

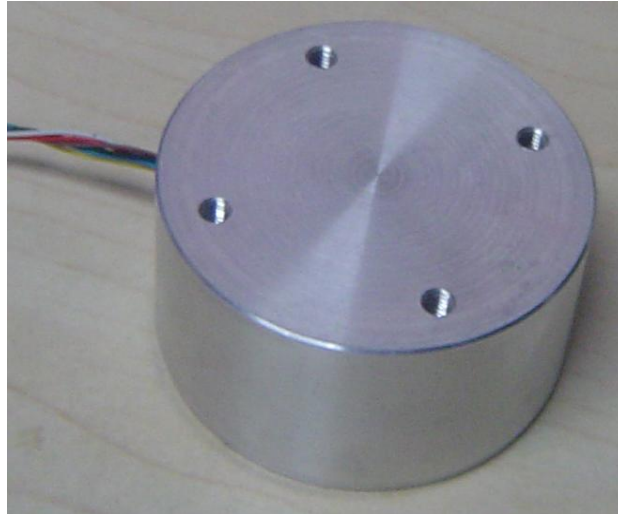


Figure 9. Comparison between the input yaw angular rate and the output yaw angular rate. B: the input of yaw angular rate; H: the output of yaw angular rate.

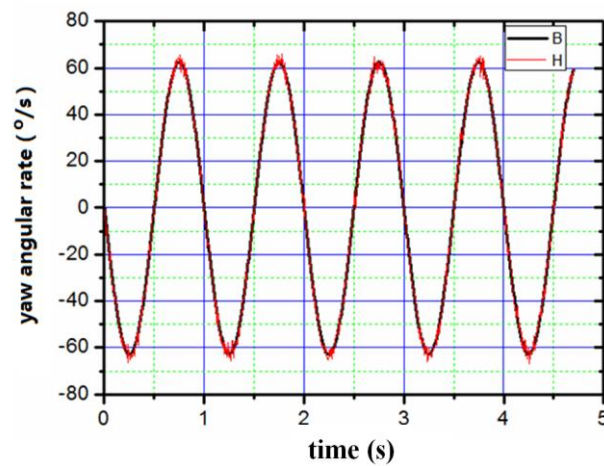


Figure 10. Comparison between the input of pitch angular rate and the output of pitch angular rate. C: the input of yaw angular rate; K: the output of yaw angular rate.

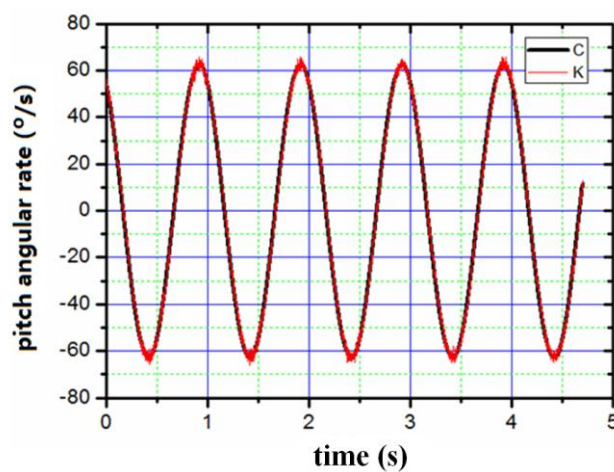
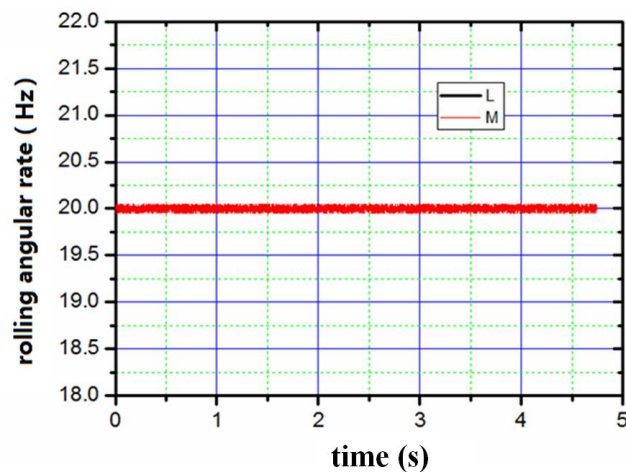


Figure 11. Comparison between the input of rolling angular rate and output of rolling angular rate. L: the input of rolling angular rate; M: the output of rolling angular rate.



The digital angular rate sensor can sense rolling, yaw and pitch angular rate of rotating carrier at one time. From Figures 9–11, it is clear that the measurement results match the actual results very well. The relative error of the sensor is less than 0.5%.

5. Conclusions

The construction, operation principles, circuits, signals processing and tests results of a novel digital angular rate sensor are described. The sensor, which has the advantages of simple structure, small size and low cost, can sense rolling rate, yaw angular rate and pitch angular rate. The experiments show that the measured angular rate (rolling, yaw and pitch angular rate) agree with the actual rate in cases of different angular rate and the max error is less than 0.5%. The effectiveness of the sensor is validated.

Acknowledgements

This project was supported by the National Natural Science Foundation of China (No. 60971024), the Program of Beijing Key Lab for Sensor (No. KF20101077202) and Key Laboratory of Modern Measurement & Control Technology (Beijing Information Science & Technology University), Ministry of Education.

References

1. Mu, S.Z.; Bu, X.Z.; Li, Y.X. Research on inertial measurement unit of high rotation vehicle. *J. Ballistics* **2006**, *8*, 88-88.
2. Lee, S.C.; Huang, Y.C. Innovative estimation method with measurement likelihood for all-accelerometer type inertial navigation system. *IEEE T. Aero. Elec. Syst.* **2002**, *38*, 339-346.
3. Qin, L.; Zhang, W.; Zhang, H.; Xu, W. Attitude measurement system based on micro-silicon accelerometer array. *Chaos, Solit. Fract.* **2006**, *29*, 141-147.
4. An, S.; Oh, Y.S.; Park, K.Y.; Lee S.S. Dual-axis microgyroscope with closed-loop detection. *Sens. Actuator. A* **1999**, *73*, 1-6.

5. Ibrahim, H.E.A. Electrostatic gyroscope pull-in study and optimum dimensions using genetic optimization. *J.Alexa. Engin.* **2005**, *44*, 845-853.
6. Gretillat, F.; Gretillat, M.A.; de Rooij, N.F. Improved design of a silicon micromachined gyroscope with piezoresistive detection and electromagnetic excitation. *J. Micro. Syst.* **1999**, *8*, 243-250.
7. Lee, S.H.; Hong, S.W.; Kim, Y.K.; Lee S.K. Planar vibratory gyroscope using electromagnetic force. *Sens. Actuator. A* **1998**, *65*, 101-108.
8. Wu, X.S; Chen, W.Y; Zhao, X.L.; Zhang, W.P. Micromachined rotating gyroscope with electromagnetically levitated rotor. *Electron. Lett.* **2006**, *42*, 912-913.
9. Bhadbhade, V; Jalili, N.; Mahmoodi, S.N. A novel piezoelectrically actuated flexural/torsional vibrating beam gyroscope. *J. Sound. Vibra.* **2008**, *311*, 1305-1324.
10. Kaqawa, Y.; Wakatsuki, N.; Takao, T.; Yoichi, T. A tubular piezoelectric vibrator gyroscope. *IEEE Sens. J.* **2006**, *2*, 325-330.
11. Wu, L.F.; Zhang, F.X. The study of the scale factor of micro-machined gyroscope. *IEICE Electron. Express* **2008**, *19*, 840-845.

© 2010 by the authors; licensee MDPI, Basel, Switzerland. This article is an open access article distributed under the terms and conditions of the Creative Commons Attribution license (<http://creativecommons.org/licenses/by/3.0/>).